MBL Lectures supplemental material

A.Scardicchio

The model

$$H = -J \sum_{i=1}^{L} \vec{s}_i \cdot \vec{s}_{i+1} - \sum_{i=1}^{L} h_i s_i^z$$

$$h_i \in [-h, h]$$

Conductance properties

$$\frac{\partial j}{\partial \mu} \sim \frac{1}{L^\gamma}$$

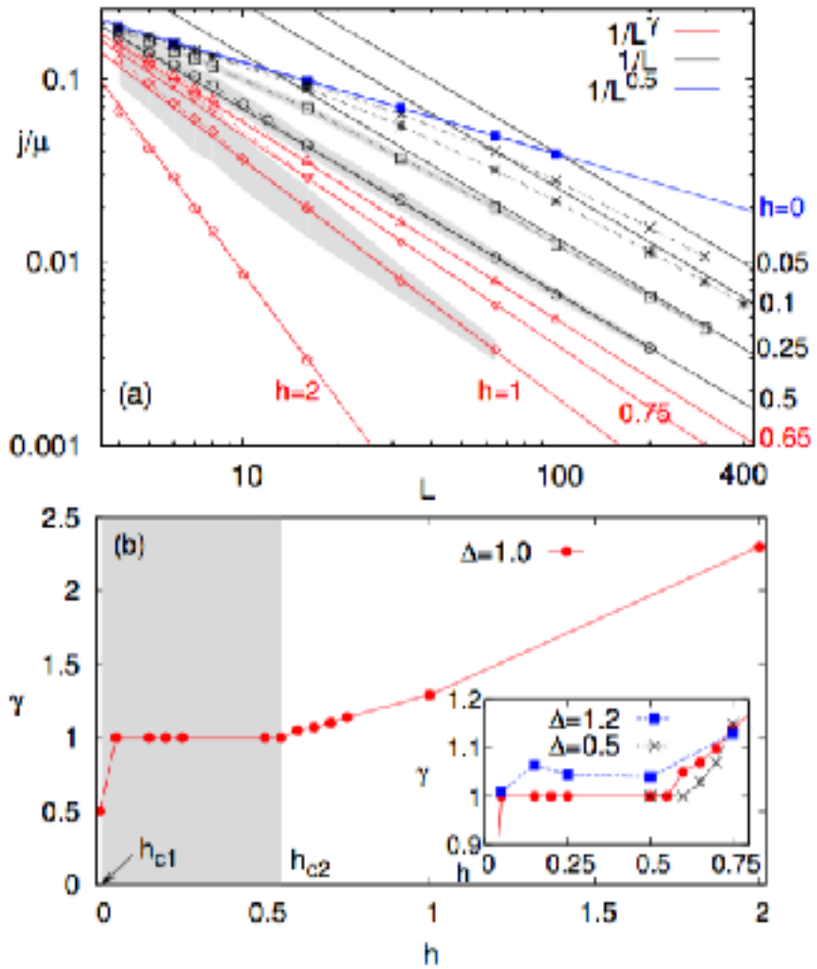

FIG. 2. (Color online) Spin transport in the ergodic phase of the Heisenberg model. (a) Scaling of the average NESS spin current j with system size, $j \sim 1/L^\gamma$, for $\Delta = 1$. Points are numerical data, lines are best fitting $1/L^\gamma$, with $\gamma = 1$ for $0 < h < h_{c2} \approx 0.55$ (black), and $\gamma > 1$ for $h_{c2} < h < h_{c3}$ (red). For $h = 1$, $h = 0.5$ and $h = 0.25$ the gray shading denotes standard deviation $\sigma(j)$ of current distribution (for $h = 0.25$ it is barely visible as it is smaller than the size of square points). (b) Dependence of γ on the disorder strength. At a critical disorder strength h_{c2} one gets a transition from diffusive to subdiffusive spin transport, while at $h_{c1} = 0$ there is a discontinuous transition from superdiffusive (for $h = 0$) to diffusive for $h_{c1} < h < h_{c2}$. Inset: similar data for $\Delta = 1.2$ and $\Delta = 0.5$.

The model

$$H = -J \sum_{i=1}^{L} \vec{s}_i \cdot \vec{s}_{i+1} - \sum_{i=1}^{L} h_i s_i^z$$

Entanglement entropy: AREA vs VOLUME

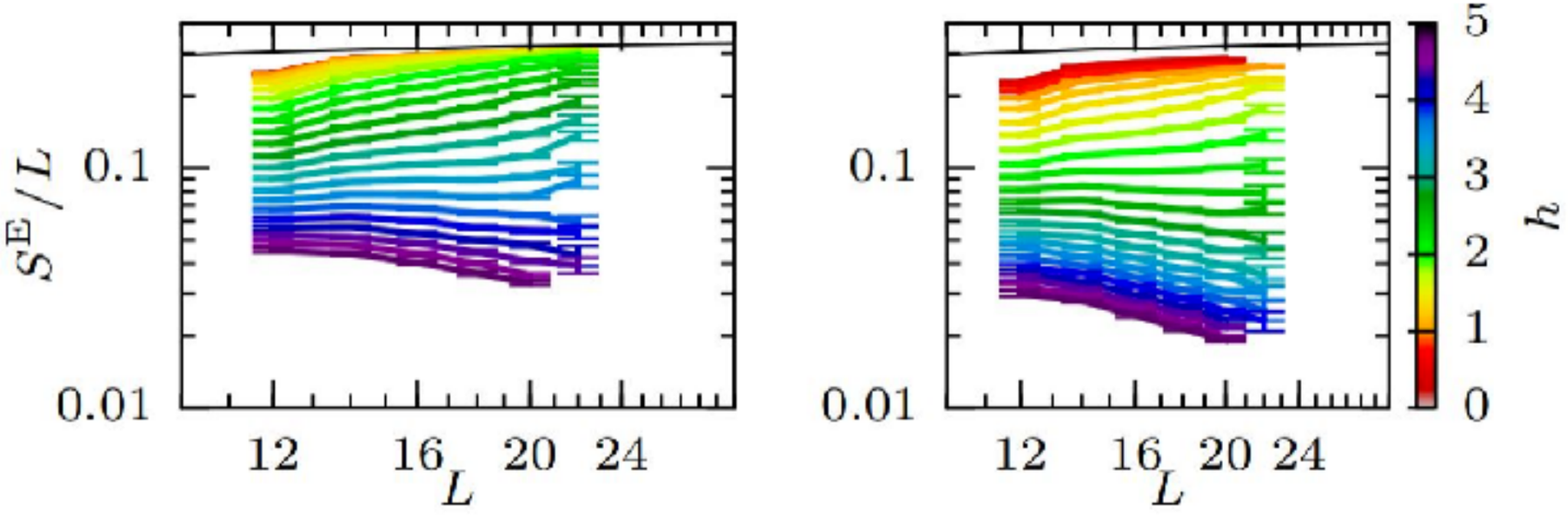

Figure 1 Bipartite entanglement entropy S^E defined in Eq. (8) for the Hamiltonian (3) with $J = J_z = 1$ and $h_a \in [-h, h]$, as a function of system size L for different disorder strengths in the middle of the spectrum (left) and in the upper part (right). For strong disorder, S^E/L decreases signaling area-law. The figure is taken from Ref. [16]

Smooth behavior of observables

Level statistics

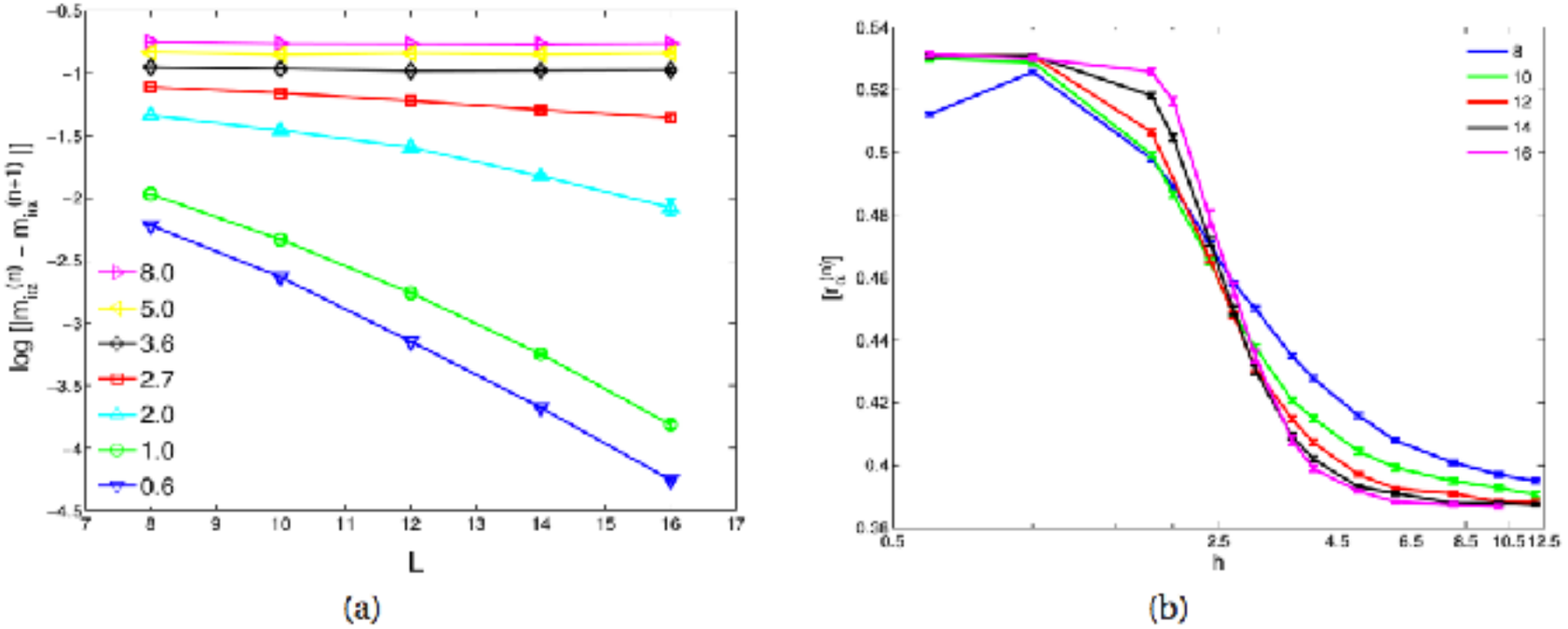

Figure 2 (a) Logarithm of the averaged difference between the local magnetizations $m_{i\alpha}^{(n)} = \langle n|S_i^z|n\rangle_\alpha$ in adjacent eigenstates of the Hamiltonian (3) with $J_z = J = 1$ and h indicated in the legend. The average is over the disorder realization α and the pairs of eigenstates. For large h, the differences remain large as the length of the chain L is increased. (b) Ratio of adjacent energy gaps defined in Eq. (10) for different system sizes L indicated in the legend. For large h, the level statistics are Poisson. Figures taken from Ref. [13]

Fraction of magnetization memory

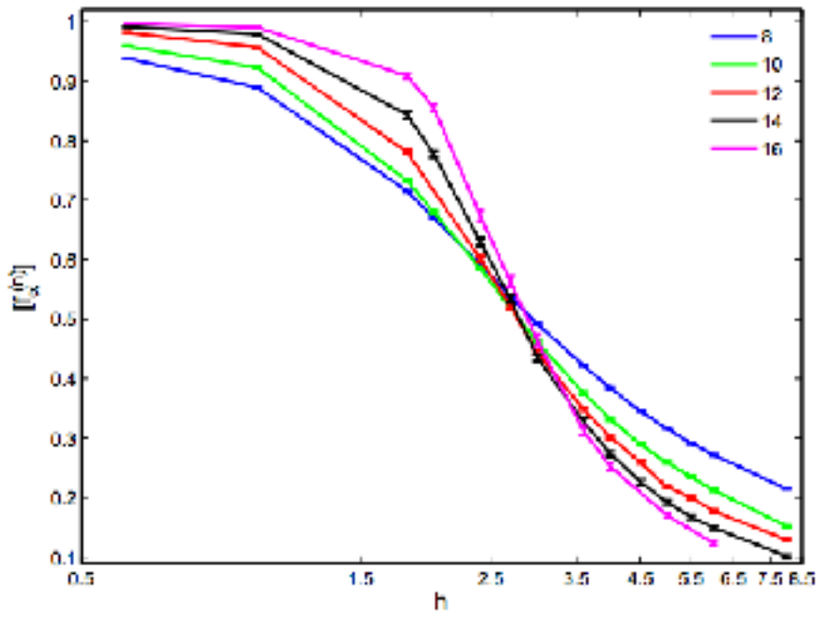

FIG. 2: (Color online) The fraction of the initial spin polarization that is dynamic (see text). The sample size L is indicated in the legend. In the ergodic phase (small h) the polarization decays substantially under the dynamics, while in the localized phase (large h) the decay is small, and this distinction gets sharper as L increases.

Logarithmic growth of Entanglement entropy

Saturation of fluctuations

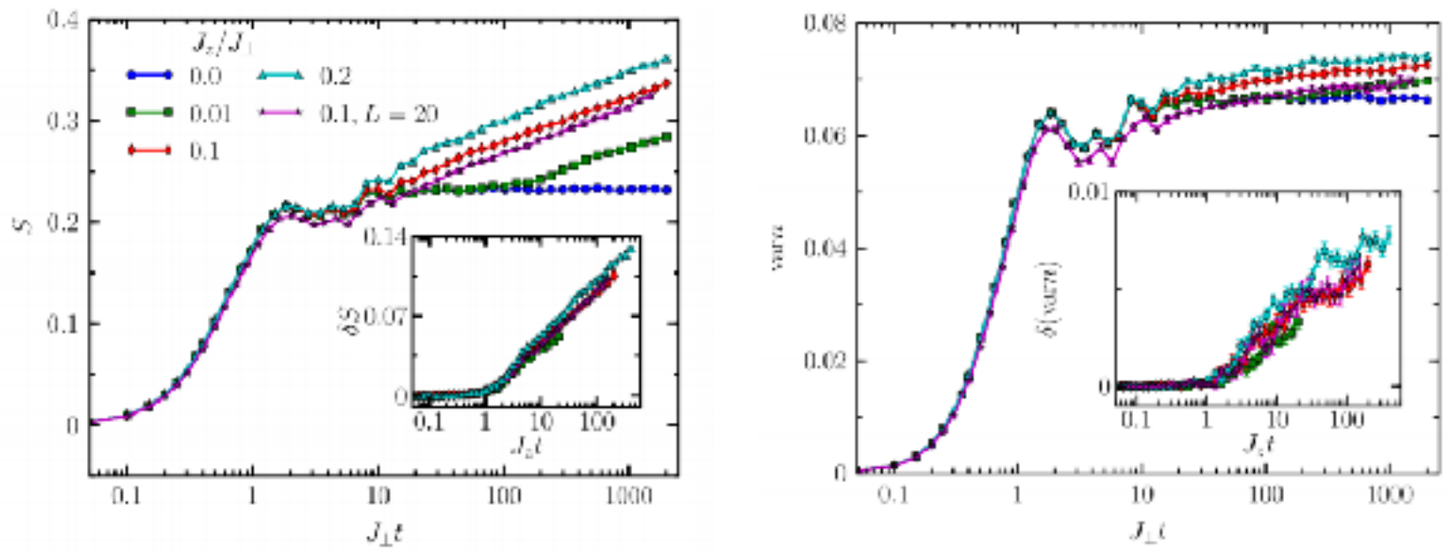

Figure 3 (a) Unbounded growth of the bipartite entanglement after a quench starting from a site-factorized S^z eigenstate of the Hamiltonian (3) with $J = J_\perp$, $h_a \in [-5, 5]$, $L = 10$ and different interaction strengths J_z. The inset shows the same data with a rescaled time axis and subtracted $J_z = 0$ values. (b) Growth of the particle number fluctuations of a half chain after the quench. The behavior is qualitatively different than the entanglement entropy: the interactions do enhance the particle number fluctuations, but while there are signs of a logarithmic growth as for the entanglement, this growth slows down with time. Figures taken from Ref. [71]

Breakdown of ETH scaling for the wave function

$$P(\psi_\sigma^n) = \left(\frac{2}{\pi N}\right)^{N/2} e^{-\sum_\sigma \frac{N}{2}(\psi_\sigma^n)^2}$$

$$x = N(\psi_\sigma^n)^2$$

independent of *N*

Ergodic

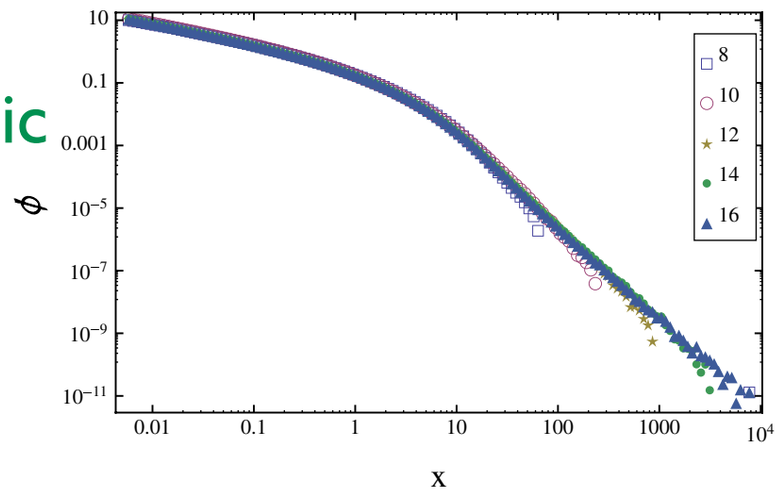

Non-ergodic

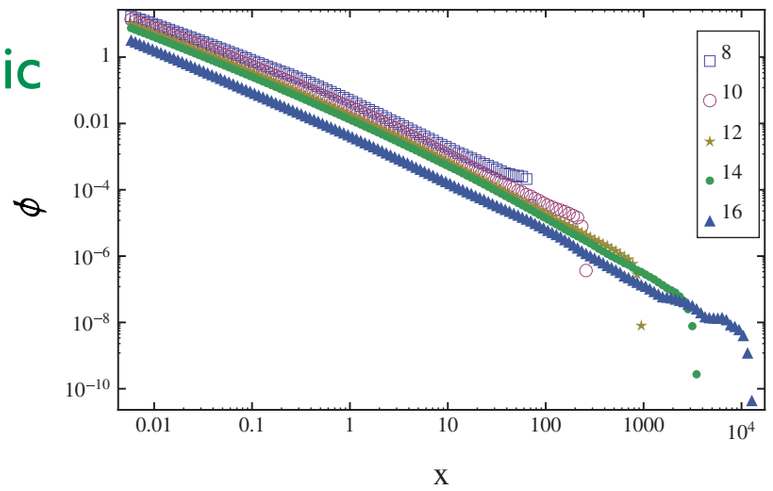

Fig. 3: (Colour on-line) The distribution ϕ of scaled wave function amplitudes $x = \mathcal{N}|\langle a|E\rangle|^2$ for different values of h. Upper panel: $h = 1.2$ in the middle of the ergodic phase where the scaling is perfectly verified; lower panel: $h = 4.2$ in the many-body localized phase. In each panel the different curves correspond to different values of N, from 8 to 16. Each curve is obtained by binning of not less than 3 10^6 squared amplitudes.